Simulation of universal optical logic gates under energy sharing collisions of Manakov solitons and fulfillment of practical optical logic criteria

M. Vijayajayanthi,[1,*] T. Kanna,[2,†] and M. Lakshmanan[3,‡]

[1]*Department of Physics, B. S. Abdur Rahman Crescent Institute of Science and Technology, Vandalur, Chennai 600 048, India*

[2]*Nonlinear Waves Research Lab, PG and Research Department of Physics, Bishop Heber College, Tiruchirapalli 620 017, India*

[3]*Department of Nonlinear Dynamics, School of Physics, Bharathidasan University, Tiruchirapalli 620 024, India*

(Received 6 July 2023; accepted 12 October 2023; published 13 November 2023)

The universal optical logic gates, namely, NAND and NOR gates, have been theoretically simulated by employing the energy sharing collision of bright optical solitons in the Manakov system, governing pulse propagation in a highly birefringent fiber. Further, we also realize the two-input optical logic gates, such as AND, OR, XOR, XNOR, for completeness of our scheme. Interestingly, our idea behind the simulation naturally satisfies all the criteria for practical optical logic, which in turn displays the strength and versatility of our theoretical simulation of universal optical logic gates. Hence, our approach paves the way for the experimentalists to create a new avenue in this direction if the energy sharing collisions of Manakov solitons are experimentally realized in the future.

DOI: 10.1103/PhysRevE.108.054213

I. INTRODUCTION

Photons can be used in the form of optical solitons to execute classical information processing and communication rather than electrons through a nonlinear medium, like highly birefringent fiber. The rapid growth in modern day information theory and the limitations on semiconductor devices, such as speed limits, energy losses, and interconnect delays, lead researchers to look for an alternate mode of technology. One such highly desirable approach is to employ all optical devices to replace the conventional integrated circuits in electronics. Light pulses are promising candidates due to their wide range of bandwidth, ultrahigh speed, low heat generation, etc. [1]. Optical logic gates serve as fundamental building blocks in such optical devices [2]. These optical logic gates could be simulated by harnessing nonlinear effects in semiconductor optical amplifier [3–5] and in photonic crystals. Interestingly, here, all the logic operations are to be performed with light in the form of solitons, nonlinear coherent structures with remarkable stability. This overcomes the demerits of present-day computers (digital electronics) such as processing speed, space, heat dissipation, etc. Realization of practical optical logic (POL) gates by employing soliton interactions is a promising effort to replace the conventional classical computers, where electrons play a major role. In recent years, many research works have been proposed and reported concerning the optical logic operations in different physical phenomena [6–12]. However, none of them have tried to verify whether they fulfill the criteria called POL.

In the present work, we theoretically propose the simulation of universal optical logic gates by making use of the rigorous asymptotic analysis of a four-soliton energy sharing collision which in turn concretely provides the mathematical support for the simulation of optical logic gates for the experimentalists. In addition to this, the input and output states of the solitons can be measured anywhere asymptotically rather than at a particular fiber distance. For demonstrative purpose, here we analyze our collision dynamics at the fiber distance $z = \pm 15$ km. Also, we propose the optical logic gates for the standard Manakov model in which there is no fiber attenuation. Even in the presence of fiber losses or attenuation, one of the authors of the present paper revealed that the energy sharing property of the Manakov solitons is preserved under strong environmental perturbations [13]. In our previous works, we theoretically explored the realization of optical single-input gates [14] and two-input gates, such as OR gate and NOR gate [15]. Here, we wish to make a proposal for all other basic two-input logic gates including the universal NAND gate. We emphasize that our theoretical approach naturally satisfies all the criteria for POL (see Sec. IV below for more details). For this purpose, we consider the incoherent propagation of two orthogonally polarized high-intense optical pulses in an elliptically birefringent fiber with high birefringence [16,17]. This type of pulse propagation is described by the following coupled nonlinear Schrödinger (CNLS) equations which can be represented by the system of coupled evolution equations [18,19]:

$$i(\Psi_{1\zeta} + \beta_{1x}\Psi_{1\tau}) - \frac{\beta_2}{2}\Psi_{1\tau\tau} + \gamma(|\Psi_1|^2 + B|\Psi_2|^2)\Psi_1 = 0, \tag{1a}$$

$$i(\Psi_{2\zeta} + \beta_{1y}\Psi_{2\tau}) - \frac{\beta_2}{2}\Psi_{2\tau\tau} + \gamma(|\Psi_2|^2 + B|\Psi_1|^2)\Psi_2 = 0, \tag{1b}$$

where ζ and τ are respectively the propagation direction and the normalized time; Ψ_j's, $j = 1$ and 2, are complex slowly

*vijayajayanthi.cnld@gmail.com

†Corresponding author: kanna_phy@bhc.edu.in

‡lakshman@cnld.bdu.ac.in

varying amplitudes; β_{1x} and β_{1y} are the inverse of the group velocities of the two modes; β_2 represents group velocity dispersion; and the effective Kerr nonlinearity coefficient γ is defined as $\frac{8n_2\omega_0}{9cA_{\rm eff}}$, where n_2 is the nonlinear index coefficient, ω_0 is the carrier frequency, and $A_{\rm eff}$ is the effective core area. Here, we have neglected the rapidly varying coherent coupling terms [19]. Furthermore, γ and β_2 are chosen to be same for both the pulses as they are at the same wavelength. The cross phase modulation (XPM) coupling parameter $B = \frac{2+2\sin^2\theta}{2+\cos^2\theta}$, where θ is the ellipticity angle which can vary between 0 and $\pi/2$. We note that in the case of linearly birefringent fiber the XPM coefficient B takes the value $2/3$ and in circularly birefringent fibers it becomes 2. In a specially fabricated elliptically birefringent fiber with ellipticity angle $\theta = 35^\circ$, one can achieve the B value as 1 [19]. Also in telecommunication fibers, the birefringence is random. In that case, B can be made to be unity. Meanwhile, the linear and nonlinear polarization mode dispersion (PMD) terms will appear [20] and therefore the coupled nonlinear Schrödinger equations can exactly be reduced to the Manakov system but with additional perturbative terms originating from the PMD. For lossless fibers, after suitable transformations, the above equation (1) can be expressed in the following dimensionless form using soliton units [16,17,19],

$$i\Psi_{1z} - \frac{\mathrm{sgn}(\beta_2)}{2}\Psi_{1tt} + \mu(|\Psi_1|^2 + B|\Psi_2|^2)\Psi_1 = 0, \quad \text{(2a)}$$

$$i\Psi_{2z} - \frac{\mathrm{sgn}(\beta_2)}{2}\Psi_{2tt} + \mu(|\Psi_2|^2 + B|\Psi_1|^2)\Psi_2 = 0, \quad \text{(2b)}$$

where the dimensionless length and the retarded time are defined as $z = \frac{\zeta}{L_D}$ and $t = \frac{T}{T_0} = (\tau - \tilde{\beta}_1\zeta)$, in which the dispersion length $L_D = \frac{T_0^2}{|\beta_2|}$, the nonlinear length $L_{\rm NL} = \frac{1}{\gamma P_0}$, and $\tilde{\beta}_1 = \frac{1}{2}(\beta_{1x} + \beta_{1y})$, with T_0 and P_0 being the initial width and the peak power, respectively, while $\mu = \frac{\gamma P_0 T_0^2}{|\beta_2|} > 0$. In the anomalous (normal) dispersion regime, $\beta_2 < 0$ (> 0), where the high-frequency (low-frequency) pulses travel faster than the low-frequency (high-frequency) pulses, the above coupled system of equations is referred to as focusing (defocusing) CNLS equations and the fiber supports bright (dark and dark-bright) solitons. These are consequences of the polarization modulation instability [21]. For the polarizing angle $\theta = 35^\circ$ (for which $B = 1$) in the anomalous dispersion regime, with a scaling transformation $z' = \frac{z}{2}$, $q_j = \sqrt{\mu}\Psi_j$, $j = 1$ and 2, and dropping the prime, we get the standard Manakov model in normalized form as follows [22],

$$iq_{1z} + q_{1tt} + 2(|q_1|^2 + |q_2|^2)q_1 = 0, \quad \text{(3a)}$$

$$iq_{2z} + q_{2tt} + 2(|q_1|^2 + |q_2|^2)q_2 = 0. \quad \text{(3b)}$$

The Manakov system (3) and its N-component generalization have been extensively studied (for details, see Refs. [22–28] and references therein). The salient attribute of this Manakov system is the interesting energy sharing collision of bright solitons as a consequence of change in the polarization vector during collision. In such energy sharing collisions, the intensity of the solitons in a given component can be suppressed (enhanced) while the other solitons experience a converse effect. Contrary to this, the solitons in the second component display a reverse scenario, thereby preserving the total intensity as well as the intensity of the individual component [23–28]. Following this, multisoliton interactions in the Manakov system have been studied by using the Hirota's bilinearization method in Refs. [25,27,28]. Recently, bound-state solitons and mutivalley dark solitons of various multicomponent CNLS-type systems have been explored by employing the Darboux transformation method [29]. The Manakov bright solitons have been first experimentally observed in the spatial domain with AlGaAs planar waveguides [30]. On the other hand, this Manakov system serves as an appropriate framework for the experimental study of modulation instability (MI) and its connection with rogue waves and different kinds of breathers, in optical fibers. In particular, an experimental configuration to realize an XPM coefficient with unity value and with very low polarization mode dispersion (PMD) [20] has been successfully demonstrated in Refs. [31] and [32] for MI studies in the Manakov system featuring anomalous and normal group velocity dispersion, respectively.

Recently, optical dark rogue waves have also been experimentally observed in the Manakov model with defocusing nonlinearity [33]. Thus, the Manakov solitons are suitable candidates for experimental realization and for further technological applications. Also, in Ref. [13], it has been clearly demonstrated that this energy sharing property of the Manakov solitons is preserved even in the presence of fiber losses. There it has been shown that for $B = 2/3$, with appropriate initial conditions, the bright solitons undergo efficient energy sharing collisions with a switching efficiency of 96%. Another interesting and detailed study on system (2) with $B = 2/3$ [34] shows that for faster colliding velocity, a similar transmission collision scenario occurs with larger (smaller) solitons becoming even larger (smaller). In our simulation procedure of logic gates, we fix a threshold level, above (below) which one shall have 1 (0) state. So, the observations in Refs. [13,34] suggest that our present approach of realizing 1 (0) logic and subsequent logic gate simulation will hold good.

II. SCHEMATIC OF FOUR-SOLITON COLLISION PROCESS

In highly birefringent fibers, it was pointed out in Ref. [25] that the bright Manakov solitons typically exhibit pairwise collision under interaction. In such a collision process, all the solitons undergo energy sharing collisions and every soliton interacts with every other soliton which is involved in the collision process. To be specific, we employ just a four-bright-soliton-collision process, in which each soliton undergoes three pairwise energy sharing interactions. One can refer to the Supplemental Material of Ref. [15] for the explicit four-soliton solution and its detailed asymptotic analysis. We denote the input solitons as unprimed solitons S_j, $j = 1, 2, 3$, and 4. We refer to the solitons emerging after the first, second, and third pairwise collisions as primed, double-primed, and triple-primed solitons, respectively. In fact S_j''' represent the output solitons. The schematic pairwise four-soliton-collision process considered in our present work is shown in Fig. 1. Here, we use the pairwise energy sharing collisions of bright Manakov solitons as such without imposing any constraints on the colliding solitons for realizing the universal logic gate.

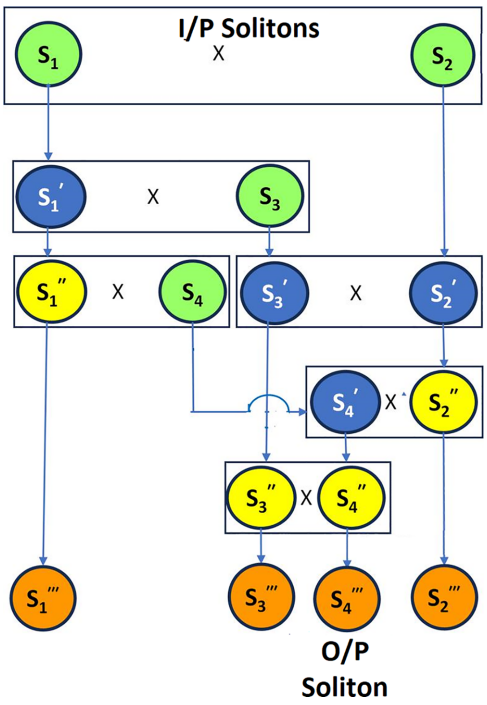

FIG. 1. Collision picture of four solitons: S_1, S_2, S_3, and S_4.

The intensities of the four colliding solitons at the input and at the output are calculated analytically from a systematic but rather lengthy asymptotic analysis.

III. NOTION BEHIND THE SIMULATION OF OPTICAL LOGIC GATES

During the energy sharing collision, the Manakov solitons experience a change in their states (polarizations) due to the enhancement or suppression of intensity which is a desirable property for performing computation. Also, it is sufficient to examine these states well before (i.e., at the input) and well after (output) collisions. The key idea is to define the asymptotic states of the jth soliton as $\rho^{j\pm} = \frac{q_1^j(z\to\pm\infty)}{q_2^j(z\to\pm\infty)} = \frac{A_1^{j\pm}}{A_2^{j\pm}}$, where $A_{1,2}^{j\pm}$ are the polarization components (1,2) of the jth soliton. Here subscripts denote the components, $+$ $(-)$ designates the state after (before) collision, and superscript j represents the soliton number. The logic gates deal with binary logic, either 1 or 0. We define such a 1 (0) state if the intensity $|\rho^{j\pm}|^2$ of the state vector exceeds (falls below) a particular reference value. For simulating the two-input logic gate, the inputs are fed into the solitons S_1 and S_2 well before interaction, and the output is taken from the soliton S_4 after interaction. The explicit forms of the states of the solitons S_1 and S_2 before interaction are

$$\rho^{1-} = \frac{\alpha_1^{(1)}}{\alpha_1^{(2)}}, \tag{4}$$

$$\rho^{2-} = \frac{A_1^{2-}}{A_2^{2-}} = \frac{N_1^{2-}}{N_2^{2-}} = \frac{\alpha_1^{(1)}\kappa_{21} - \alpha_2^{(1)}\kappa_{11}}{\alpha_1^{(2)}\kappa_{21} - \alpha_2^{(2)}\kappa_{11}}, \tag{5}$$

where

$$\kappa_{il} = \frac{\sum_{n=1}^{2}\alpha_i^{(n)}\alpha_l^{(n)*}}{(k_i + k_l^*)}, \quad i, l = 1, 2, 3, 4.$$

Similarly, the state of the soliton S_4 after collision is given by $\rho^{4+} = \frac{\alpha_4^{(1)}}{\alpha_4^{(2)}}$. In the above equations, $\alpha_l^{(m)}$ ($l = 1$, 2, and 4; $m = 1$ and 2) represent the polarization parameters of solitons S_1, S_2, and S_4 and they can take any arbitrary complex value. The other quantities, κ_{11}, κ_{21}, and κ_{12}, are defined by the soliton parameters α and k. Though the third soliton S_3 does not explicitly appear in the above expressions, it indirectly influences the energy sharing collisions. The ratio of intensities of two components for the solitons S_1 and S_2 before interaction as well as that for soliton S_4 after interaction can be obtained by taking the absolute squares of these complex states and they are given by $|\rho^{1-}|^2$, $|\rho^{2-}|^2$, and $|\rho^{4+}|^2$, respectively. Hence, one can measure the ratio of the intensities of the two components for the input and output solitons analytically from the asymptotic analysis. Then as mentioned before if the ratio of intensities of two components for a given soliton S_j is greater (less) than some specific threshold value, say 1, before interaction, then we denote the input state of that soliton S_j as the "1(0)″ state. Thus the 1(0) state of a particular soliton S_j corresponds to $|\rho^{j-}|^2 > 1 (< 1)$.

IV. CRITERIA FOR PRACTICAL OPTICAL LOGIC AND THEIR FULFILLMENT

The article by Miller [35] lays out nicely the relevant criteria for optical logic, such as cascadability, fan-out, logic-level restoration, input and output isolation, critical biasing, and independence of loss. All these requirements are naturally met by the proposed soliton-collision-based computing. As a result, the scheme does stand out in a way against a myriad of other nonlinear switching schemes. Below, we discuss all the criteria in detail, in the framework of soliton collision.

(i) Fan-out. In a four-soliton-collision process, if the input state is assigned to the soliton 1 (S_1) before collision, then it can be switched to the output of any of the other two solitons after collision, say solitons S_2 and S_4, by appropriately imposing conditions on the soliton parameters. This essentially implies the process of fan-out which indicates the state of one soliton (S_1) before collision is used to drive as an input to at least two different solitons (S_2 and S_4) after collision. To facilitate our understanding, we consider the following example. The parametric values to drive the 0 input state to solitons S_2 and S_4 are chosen as $k_1 = 1 + i$, $k_2 = 1.2 + 0.5i$, $k_3 = 0.9 - 0.5i$, $k_4 = 1.3 - i$, $\alpha_1^{(1)} = 2$, $\alpha_1^{(2)} = 6$, $\alpha_2^{(2)} = 1 - i$, $\alpha_3^{(1)} = 2$, $\alpha_3^{(2)} = 1$, and $\alpha_4^{(2)} = 2 - i$. The parametric values of $\alpha_4^{(1)}$ and $\alpha_2^{(1)}$ are determined as $0.6 - 0.3i$ and $0.002 - 0.4i$, respectively, from the following conditions:

$$\alpha_4^{(1)} = \frac{\alpha_1^{(1)}\alpha_4^{(2)}}{\alpha_1^{(2)}}, \tag{6}$$

$$\frac{N_1^{2+}}{N_2^{2+}} - \frac{\alpha_4^{(1)}}{\alpha_4^{(2)}} = 0. \tag{7}$$

The expressions for N_1^{2+} and N_2^{2+} are already given in the asymptotic analysis (see, the Supplemental Material of Ref. [15]). In order to drive the 1 input state of the soliton S_1 to the solitons S_2 and S_4, we have to choose the soliton S_1 parameters as $\alpha_1^{(1)} = 6$ and $\alpha_1^{(2)} = 2$. From the above conditions, the parameters $\alpha_4^{(1)}$ and $\alpha_2^{(1)}$ are evaluated as $6 - 3i$ and

TABLE I. Truth table.

Input S_1	Output 1 S_2'''	Output 2 S_4'''
0	0	0
1	1	1

TABLE II. Intensity table.

Input S_1	Output 1 S_2'''	Output 2 S_4'''
0.1	0.1	0.1
9	9	9

$3.4 - 0.8i$ and all the other parameters are as same as those for the 0 state. The fanning out of the input states is clearly given in Tables I and II. Figures 2 and 3 depict the fanning out of input states 0 and 1, respectively.

(ii) Logic-level restoration. Here the optical pulses are propagating in the form of solitons which is by nature a localized coherent structure that can travel over long distances without alteration in shape and is robust against strong environmental perturbations. This special property of solitons can restore the logic signal throughout its propagation in an optical fiber.

(iii) Input and output isolation. In the realization of optical logic gates, the inputs are fed into the first two pulses before collision, say soliton S_1 and soliton S_2, respectively. Then the output is measured in the last pulse after collision (total of four solitons involved in the composite collision), say soliton S_4. This final soliton is well separated from the input soliton. Hence, the input and output solitons are treated separately, which will prevent the input pulses from being reflected back into the output pulse.

(iv) Logic level independent of loss. To achieve this, we need a differential signaling that requires the ratios of powers or difference of powers at the input. Interestingly, in our present work, indeed we define the state of a particular soliton as the ratio of the intensities of the soliton propagating in the two components. For example,

$$|\rho^1|^2 = \frac{|A_1^1|^2}{|A_2^1|^2}, \tag{8}$$

where $|\rho^1|^2$ represents the state of the soliton S_1, $|A_1^1|^2$ represents the intensity of the soliton S_1 propagating in the q_1 mode, and $|A_2^1|^2$ denotes the intensity of the soliton S_1 propagating in the q_2 mode. Thus, we have taken the ratio of intensities of the solitons propagating in two different modes (q_1 and q_2) to represent the state of a particular soliton, say soliton S_1. This automatically satisfies the differential signaling criteria in Ref. [35].

(v) Absence of critical biasing. In order to achieve 1(0) states, we do not require a precise value of ratio of intensities of two components for the solitons. Rather, one can fix an arbitrary threshold value above (below) which all the values of intensities can be treated as 1(0) states. Specifically, we are considering 1(0) states which are having $|\rho|^2$ values above (below) a threshold. And hence, there is no need for high precision for the states. In this way, we introduce the absence of critical biasing in the soliton-collision-based optical computing.

(vi) Cascadability. We employ the four-soliton-collision process for the simulation of the NOR gate in the present paper. However, in our earlier work [14], we have demonstrated the simulation of one input gates such as the COPY gate, the NOT gate, and the ONE gate by employing a three-soliton-collision process. Here the input is fed into the second soliton S_2 before collision and the output is taken up from the third soliton S_3 after collision.

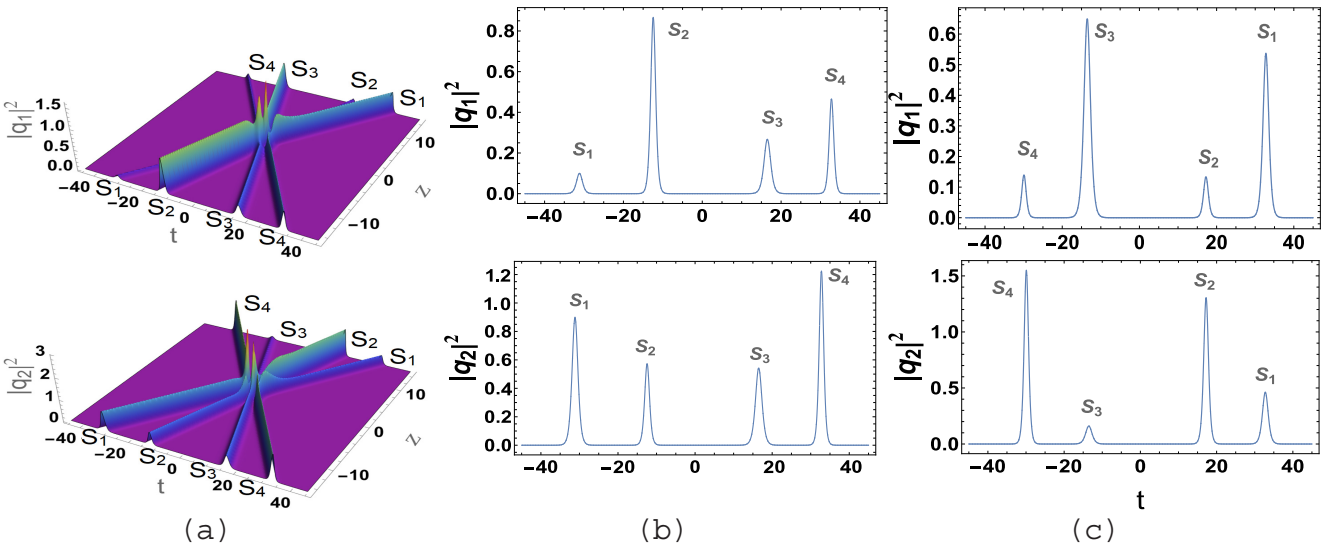

FIG. 2. Fan-out gate. The state of the input soliton (S_1) is 0, and the states of the output solitons (S_2 and S_4) are 0 and 0. Panel (a) displays the mesh plots of the intensity profiles while panels (b) and (c) depict the two-dimensional plots of intensities at the input ($z = -15$) and at the output ($z = 15$), respectively.

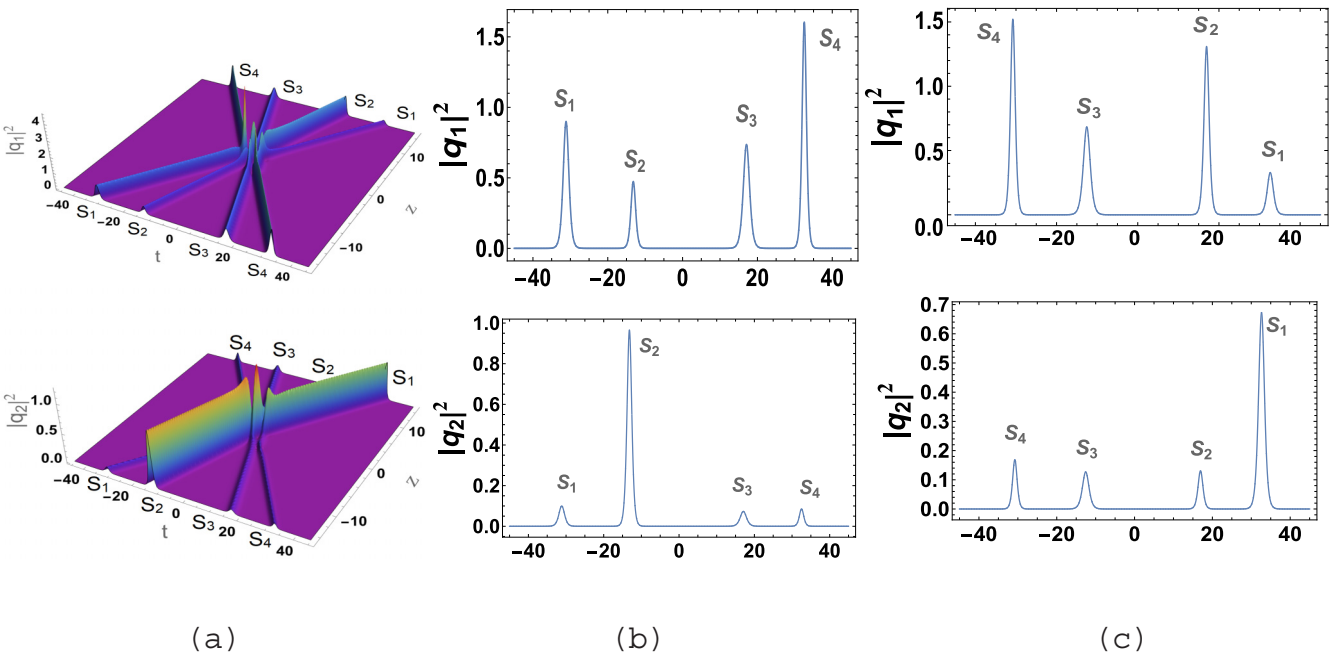

FIG. 3. Fan-out gate. The state of the input soliton (S_1) is 1, and the states of the output solitons (S_2 and S_4) are 1 and 1. Panel (a) displays the mesh plots of the intensity profiles while panels (b) and (c) depict the two-dimensional plots of intensities at the input ($z = -15$) and at the output ($z = 15$), respectively.

In the present paper, it is shown that for the simulation of the NOR gate, the inputs are fed into the solitons S_1 and S_2 before collision and the output is taken up from soliton S_4 after collision. Instead, in order to use the criteria of cascadability, one can use the output of the one-input gate, say the COPY gate (which can be realized from the three-soliton collision), and S_3'' as one of the inputs to the universal NOR gate, whereas the first soliton S_1 can be treated as another input, while the output is taken up from soliton S_4 as usual. In a nutshell, we may claim that one can simulate the two-input gate (universal gate) by cascading the output of the one-input gate.

Thus, the fulfillment of POL by our present proposed work and the experiments on Manakov solitons and their energy sharing collisions [32,36] demonstrate the definite possibility to simulate optical logic gates satisfying POL. This is an important advancement in soliton-collision-based computing.

V. SIMULATION OF TWO-INPUT OPTICAL LOGIC GATES USING FOUR-SOLITON COLLISIONS

In this section, we demonstrate the simulation of all the two-input optical logic gates, including universal gates such as the NAND, NOR, AND, OR, XOR, and XNOR gates, from out of the four-soliton-collision process.

A. NAND gate

To achieve the required output corresponding to the NAND gate, we deduce the following condition on the soliton parameters from asymptotic analysis:

$$\alpha_4^{(2)} = \left(\frac{\alpha_1^{(1)}}{\alpha_1^{(2)}} \times \frac{\alpha_2^{(1)}\left((k_1 - k_2)\left|\alpha_1^{(1)}\right|^2 - (k_2 + k_1^*)\left|\alpha_1^{(2)}\right|^2\right) + (k_1 + k_1^*)\alpha_1^{(1)}\alpha_1^{(2)*}\alpha_2^{(2)}}{(k_1 + k_1^*)\alpha_1^{(1)*}\alpha_2^{(1)}\alpha_1^{(2)} - \alpha_2^{(2)}\left((k_2 - k_1)\left|\alpha_1^{(2)}\right|^2 + (k_2 + k_1^*)\left|\alpha_1^{(1)}\right|^2\right)} \right) \alpha_4^{(1)}. \tag{9}$$

The above relation (9) is obtained by imposing the condition $\rho^{4+} = (\rho^{1-}\rho^{2-})^{-1}$ on the state vectors of the input solitons (S_1, S_2) and the output soliton (S_4) so that the Boolean algebra of the NAND gate is satisfied. Assigning (0,0) input states to (S_1, S_2) by choosing $\alpha_1^{(1)} = 2$, $\alpha_1^{(2)} = 6$, $\alpha_2^{(1)} = 2$, and $\alpha_2^{(2)} = 5$, we achieve the 1 output state from soliton S_4 for the parameter choices $k_1 = 0.5 + i$, $k_2 = 1 + 0.5i$, $k_3 = 0.9 - 0.5i$, $k_4 = 1.3 - i$, $\alpha_3^{(1)} = 3$, $\alpha_3^{(2)} = 1$, and $\alpha_4^{(1)} = 0.1 - 0.2i$ along with the condition (9), which is depicted in Fig 4. Assigning (0,1) input states to (S_1, S_2) by choosing $\alpha_1^{(1)} = 2$, $\alpha_1^{(2)} = 6$, $\alpha_2^{(1)} = 50$, and $\alpha_2^{(2)} = 45$, we achieve the 1 output state from soliton S_4. All the other soliton parameters are chosen to be the same as those above for all the combinations of input states. The (1,0) input states are fed into the solitons (S_1, S_2) by choosing $\alpha_1^{(1)} = 11$, $\alpha_1^{(2)} = 2$, $\alpha_2^{(1)} = 2$, and $\alpha_2^{(2)} = 5$, so that we achieve the 1 output state from soliton S_4. Assigning (1,1) input states to (S_1, S_2) by choosing $\alpha_1^{(1)} = 9$, $\alpha_1^{(2)} = 2$,

TABLE III. Truth table of the NAND gate.

Input 1 (S_1)	Input 2 (S_2)	Output (S_4'')
0	0	1
0	1	1
1	0	1
1	1	0

TABLE IV. Intensity table of the NAND gate.

Input 1 $\lvert\rho^{1-}\rvert^2$	Input 2 $\lvert\rho^{2-}\rvert^2$	Output $\lvert\rho^{4+}\rvert^2$
0.1	0.2	33
0.1	7	1.6
24	0.02	1.8
23	32	0.005

$\alpha_2^{(1)} = 7$, and $\alpha_2^{(2)} = 1.5$, we achieve the 0 output state from soliton S_4. The truth table and the corresponding intensity tables (calculated values of the ratios of intensities of solitons) are given in Tables III and IV. The other universal gate, namely the NOR gate, has already been demonstrated in our recent work [15].

B. AND gate

As discussed in the NAND gate, here we deduce the following condition on the soliton parameters from asymptotic analysis in order to achieve the required output corresponding to the AND gate:

$$\alpha_4^{(1)} = \left(\frac{\alpha_1^{(1)}}{\alpha_1^{(2)}} \times \frac{\alpha_2^{(1)}\left((k_1-k_2)\left|\alpha_1^{(1)}\right|^2 - (k_2+k_1^*)\left|\alpha_1^{(2)}\right|^2\right) + (k_1+k_1^*)\alpha_1^{(1)}\alpha_1^{(2)*}\alpha_2^{(2)}}{(k_1+k_1^*)\alpha_1^{(1)*}\alpha_2^{(1)}\alpha_1^{(2)} - \alpha_2^{(2)}\left((k_2-k_1)\left|\alpha_1^{(2)}\right|^2 + (k_2+k_1^*)\left|\alpha_1^{(1)}\right|^2\right)}\right)\alpha_4^{(2)}. \tag{10}$$

The above relation (10) is obtained by imposing the condition $\rho^{4+} = \rho^{1-}\rho^{2-}$ on the state vectors of the input solitons (S_1, S_2) and the output soliton (S_4) so that the Boolean algebra of the AND gate is satisfied. Now, assigning (0,0) input states to (S_1, S_2) by choosing $\alpha_1^{(1)} = 2$, $\alpha_1^{(2)} = 6$, $\alpha_2^{(1)} = 2$, and $\alpha_2^{(2)} = 5$, we achieve the 0 output state from soliton S_4 for the parameter choices $k_1 = 0.5 + i$, $k_2 = 1 + 0.5i$, $k_3 = 0.9 - 0.5i$, $k_4 = 1.3 - i$, $\alpha_3^{(1)} = 3$, $\alpha_3^{(2)} = 1$, and $\alpha_4^{(2)} = 0.001 - 0.002i$ along with the condition (10), which is depicted in Fig. 5. For the (0,1) input states of the solitons (S_1, S_2), we obtain the 0 output state from soliton S_4 by choosing $\alpha_1^{(1)} = 2$, $\alpha_1^{(2)} = 6$, $\alpha_2^{(1)} = 50$, and $\alpha_2^{(2)} = 45$. All the other soliton parameters are

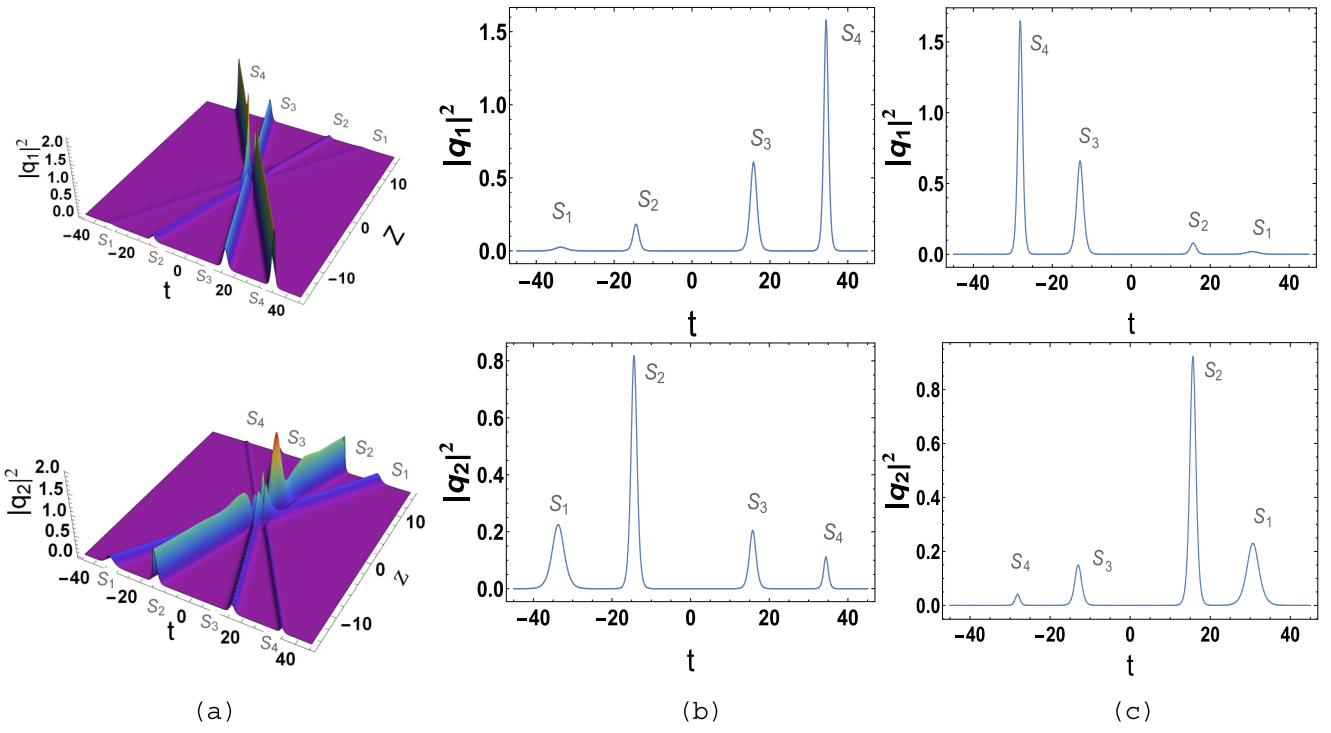

FIG. 4. NAND gate. The states of the input solitons (S_1 and S_2) are 0 and 0, and the state of the output soliton (S_4) is 1. Panel (a) displays the mesh plots of the intensity profiles while panels (b) and (c) depict the two-dimensional plots of intensities at the input ($z = -15$) and at the output ($z = 15$), respectively.

TABLE V. Truth table of the AND gate.

Input 1 (S_1)	Input 2 (S_2)	Output (S_4'')
0	0	0
0	1	0
1	0	0
1	1	1

TABLE VI. Intensity table of the AND gate.

Input 1 $\lvert\rho^{1-}\rvert^2$	Input 2 $\lvert\rho^{2-}\rvert^2$	Output $\lvert\rho^{4+}\rvert^2$
0.1	0.2	0.03
0.1	6.9	0.6
7.6	0.02	0.2
23	21	165

chosen to be the same as those above for all other combinations of input states. Assigning (1,0) input states to (S_1, S_2) by choosing $\alpha_1^{(1)} = 6$, $\alpha_1^{(2)} = 2$, $\alpha_2^{(1)} = 2$, and $\alpha_2^{(2)} = 5$, we achieve the 0 output state from soliton S_4. Finally, (1,1) input states are given to the solitons (S_1, S_2) by choosing $\alpha_1^{(1)} = 9$, $\alpha_1^{(2)} = 2$, $\alpha_2^{(1)} = 7$, and $\alpha_2^{(2)} = 1.5$, and we obtain the 1 output state from soliton S_4. The truth table and the corresponding intensity tables are given in Tables V and VI.

The detailed demonstration of the OR logic gate is discussed in the Supplemental Material of our recent work [15].

C. XOR gate

To simulate the XOR gate, two inputs are fed into solitons S_1 and S_2 and the output is taken up from soliton S_4, as usual. In order to get the desired output satisfying the truth table of the XOR gate, we make use of the condition $\rho^{4+} = \rho^{1-} - \rho^{2-}$ and choose

$$\alpha_4^{(1)} = \left(\frac{\alpha_1^{(1)}}{\alpha_1^{(2)}} - \frac{\alpha_2^{(1)}\left((k_1 - k_2)\left|\alpha_1^{(1)}\right|^2 - (k_2 + k_1^*)\left|\alpha_1^{(2)}\right|^2\right) + (k_1 + k_1^*)\alpha_1^{(1)}\alpha_1^{(2)*}\alpha_2^{(2)}}{(k_1 + k_1^*)\alpha_1^{(1)*}\alpha_2^{(1)}\alpha_1^{(2)} - \alpha_2^{(2)}\left((k_2 - k_1)\left|\alpha_1^{(2)}\right|^2 + (k_2 + k_1^*)\left|\alpha_1^{(1)}\right|^2\right)}\right)\alpha_4^{(2)}. \tag{11}$$

Assigning the (0,0) input states to (S_1, S_2) by choosing $\alpha_1^{(1)} = 2$, $\alpha_1^{(2)} = 6$, $\alpha_2^{(1)} = 2$, and $\alpha_2^{(2)} = 5$, we achieve the 0 output state from soliton S_4 for the parameter choices $k_1 = 0.5 + i$, $k_2 = 1 + 0.5i$, $k_3 = 0.9 - 0.5i$, $k_4 = 1.3 - i$, $\alpha_3^{(1)} = 3$, $\alpha_3^{(2)} = 1$, and $\alpha_4^{(2)} = 2 - i$ along with the condition (11), which is shown in Fig 6. Likewise, setting the (0,1) input states to (S_1, S_2) by choosing $\alpha_1^{(1)} = 2$, $\alpha_1^{(2)} = 6$, $\alpha_2^{(1)} = 5$, and $\alpha_2^{(2)} = 2$, we achieve the 1 output state from soliton S_4 for the above parameter choices. All the other soliton parameters are the same as those mentioned above for all the other combinations of input. Assigning (1,0) input states to (S_1, S_2) by choosing $\alpha_1^{(1)} = 6$, $\alpha_1^{(2)} = 2$, $\alpha_2^{(1)} = 2$, and $\alpha_2^{(2)} = 5$, we achieve the 1 output state from soliton S_4 for the above parameter choices. Finally, the (1,1) input states are fed into the solitons (S_1, S_2)

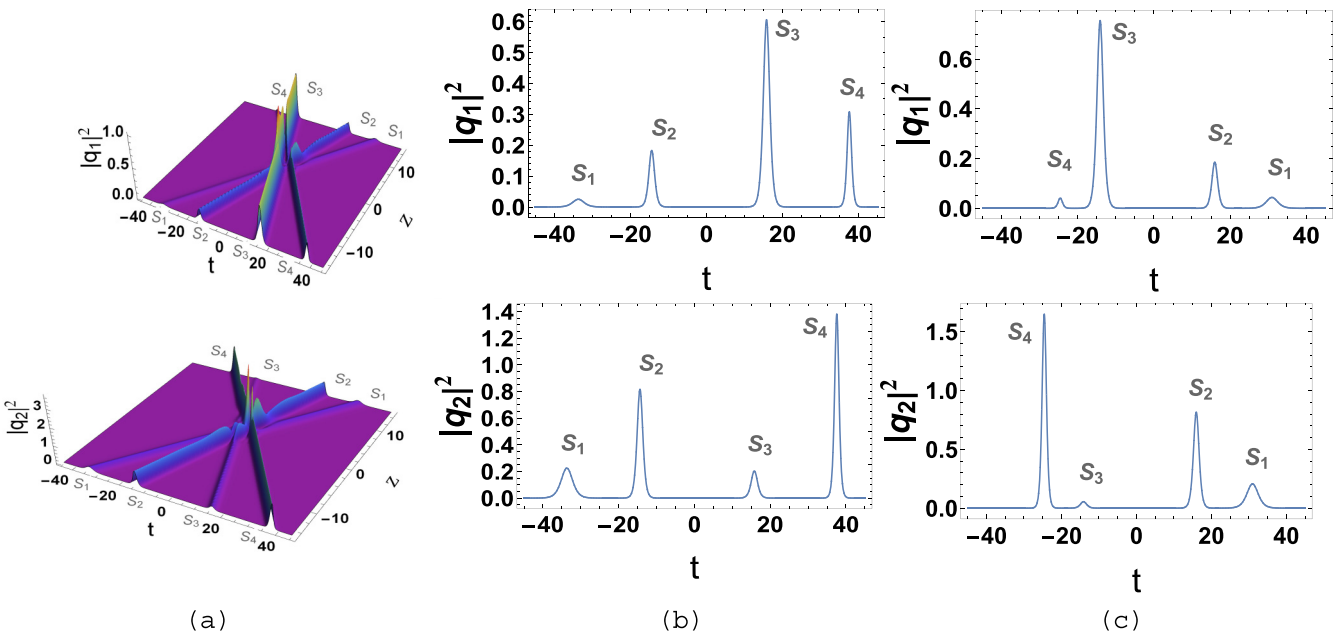

FIG. 5. AND gate. The states of the input solitons (S_1 and S_2) are 0 and 0, and the state of the output soliton (S_4) is 0. Panel (a) displays the mesh plots of the intensity profiles while panels (b) and (c) depict the two-dimensional plots of intensities at the input ($z = -15$) and at the output ($z = 15$), respectively.

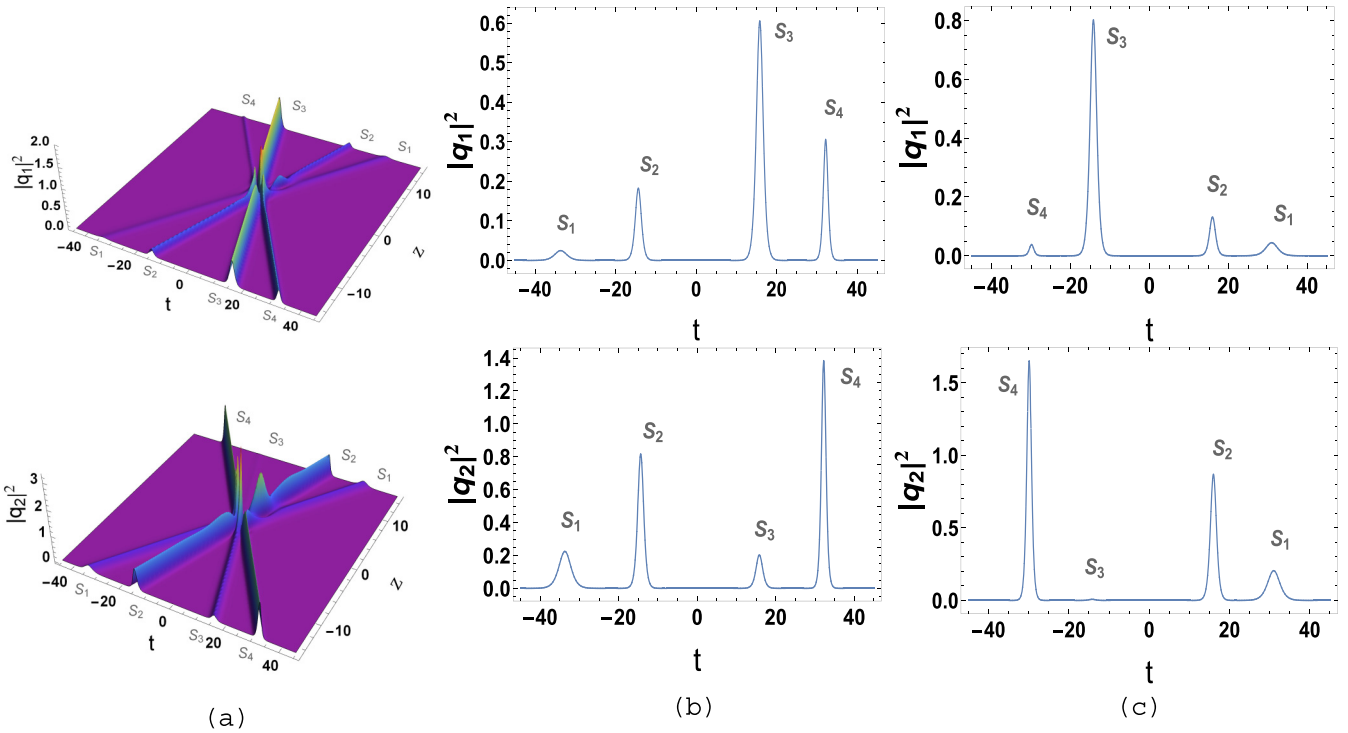

FIG. 6. XOR gate. The states of the input solitons (S_1 and S_2) are 0 and 0, and the state of output soliton (S_4) is 0. Panel (a) displays the mesh plots of the intensity profiles while panels (b) and (c) depict the two-dimensional plots of intensities at the input ($z = -15$) and at the output ($z = 15$), respectively.

by choosing $\alpha_1^{(1)} = 6$, $\alpha_1^{(2)} = 2$, $\alpha_2^{(1)} = 5$, and $\alpha_2^{(2)} = 2$, and we achieve the 0 output state from soliton S_4 for the parameter choices. Tables VII and VIII provide the truth table and the corresponding intensity table of the XOR gate, respectively.

D. XNOR gate

In order to get the desired output satisfying the truth table of the XNOR gate, we make use of the condition $\rho^{4+} = (\rho^{1-} - \rho^{2-})^{-1}$ and choose

$$\alpha_4^{(2)} = \left(\frac{\alpha_1^{(1)}}{\alpha_1^{(2)}} - \frac{\alpha_2^{(1)}\left((k_1 - k_2)\left|\alpha_1^{(1)}\right|^2 - (k_2 + k_1^*)\left|\alpha_1^{(2)}\right|^2\right) + (k_1 + k_1^*)\alpha_1^{(1)}\alpha_1^{(2)*}\alpha_2^{(2)}}{(k_1 + k_1^*)\alpha_1^{(1)*}\alpha_2^{(1)}\alpha_1^{(2)} - \alpha_2^{(2)}\left((k_2 - k_1)\left|\alpha_1^{(2)}\right|^2 + (k_2 + k_1^*)\left|\alpha_1^{(1)}\right|^2\right)} \right) \alpha_4^{(1)}. \tag{12}$$

Setting the (0,0) input states to (S_1, S_2) by choosing $\alpha_1^{(1)} = 2$, $\alpha_1^{(2)} = 6$, $\alpha_2^{(1)} = 2$, and $\alpha_2^{(2)} = 5$, we achieve the 1 output state from soliton S_4 for the parameter choices $k_1 = 0.5 + i$, $k_2 = 1 + 0.5i$, $k_3 = 0.9 - 0.5i$, $k_4 = 1.3 - i$, $\alpha_3^{(1)} = 3$, $\alpha_3^{(2)} = 1$, and $\alpha_4^{(1)} = 2 - i$ along with the condition (12), which is depicted in Fig 7. Assigning the (0,1) input states to (S_1, S_2) by choosing $\alpha_1^{(1)} = 2$, $\alpha_1^{(2)} = 6$, $\alpha_2^{(1)} = 5$, and $\alpha_2^{(2)} = 2$, we obtain the 0 output state from soliton S_4 for the above parameter choices. All the other soliton parameters are the same as those mentioned above for all the other combinations of input. The (1,0) input states are fed into the solitons (S_1, S_2) by choosing $\alpha_1^{(1)} = 6$, $\alpha_1^{(2)} = 2$, $\alpha_2^{(1)} = 2$, and $\alpha_2^{(2)} = 5$, and we achieve the 0 output state from the soliton S_4 for the parameter choices. Finally the (1,1) input states are given to the solitons (S_1, S_2) by choosing $\alpha_1^{(1)} = 6$, $\alpha_1^{(2)} = 2$, $\alpha_2^{(1)} = 5$, and $\alpha_2^{(2)} = 2$, and we obtain the 1 output state from the soliton

TABLE VII. Truth table of the XOR gate.

Input 1 (S_1)	Input 2 (S_2)	Output (S_4''')
0	0	0
0	1	1
1	0	1
1	1	0

TABLE VIII. Intensity table of the XOR gate.

Input 1 $\lvert\rho^{1-}\rvert^2$	Input 2 $\lvert\rho^{2-}\rvert^2$	Output $\lvert\rho^{4+}\rvert^2$
0.08	0.2	0.02
0.1	49	54
8	0.03	10
7.6	4.5	0.9

TABLE IX. Truth table of the XNOR gate.

Input 1 (S_1)	Input 2 (S_2)	Output (S_4'')
0	0	1
0	1	0
1	0	0
1	1	1

TABLE X. Intensity table of the XNOR gate.

Input 1 $\lvert\rho^{1-}\rvert^2$	Input 2 $\lvert\rho^{2-}\rvert^2$	Output $\lvert\rho^{4+}\rvert^2$
0.13	0.2	41
0.14	32	0.02
7.6	0.03	0.1
7	5	1.1

S_4 for the above parameter choices. The truth table and the corresponding intensity tables of the XNOR gate are given inTables IX and X, respectively.

VI. CONCLUSION

We have theoretically demonstrated the simulation of optical universal logic gates, namely, the NAND and NOR gates, using the energy sharing collision of four bright solitons in a randomly varying highly birefringent fiber described by the Manakov system. For completeness of our study, we have also simulated the AND, OR, XOR, and XNOR optical logic gates. The greatest advantage of our present work is that the notion behind the simulation of two-input logic gates satisfies all the criteria for practical optical logic. One can extend the work to realize flip flops, half adder and full adder, etc. The same theoretical realization of universal gates may be accomplished by using bound solitons in the future. Work is in progress in this direction and it paves the way to simulate multistate logic and memory-storage devices. We hope that the present research work will insightful for the experimentalists who are interested in realizing the energy sharing collision of solitons.

ACKNOWLEDGMENTS

M.V. thanks the Management at B. S. Abdur Rahman Crescent Institute of Science and Technology for the extended support. T.K. acknowledges the support received from SERB, Department of Science and Technology, Government of India, through a Core Research Grant (Grant No. CRG/2021/004119). M.L. wishes to acknowledge the financial support under the DST-SERB National Science Chair position awarded to him.

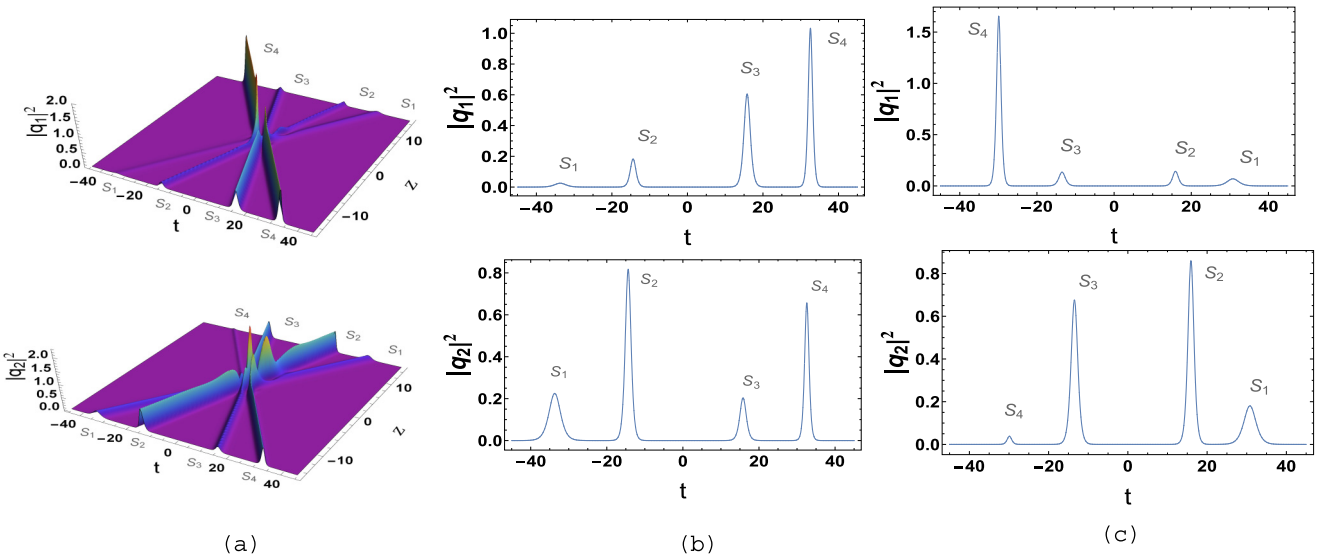

FIG. 7. XNOR gate: The state of input solitons (S_1 and S_2) are "0″ and "0″ and the state of output soliton (S_4) is "1″. The first column (a) displays the mesh plots of the intensity profiles while the middle and last columns (b) and (c) depict the two-dimensional plots of intensities at the input ($z = -15$) and at the output ($z = 15$), respectively.

[1] R. Tucker, Nat. Photonics **4**, 405 (2010).
[2] E. G. Anagha and R. K. Jeyachitra, Opt. Eng. **61**, 060902 (2022).
[3] T. Durhuus, B. Fernier, P. Garabedian, F. Leblond, J. L. Lafragette, B. Mikkelsen, C. G. Joergensen, and K. E. Stubkjaer, in *Conference on Lasers and Electro-Optics*, edited by A. Johnson, R. Lind, T. Baer, and A. Smirl, Vol. 12 of OSA Technical Digest (Optica Publishing Group, 1992), paper CThS4.
[4] H. Soto, C. A. Diaz, J. Topomondzo, D. Erasme, L. Schares, and G. Guekos, IEEE Photonics Technol. Lett. **14**, 498 (2002).
[5] B. Han and Y. Liu, AIP Adv. **9**, 015007 (2019).
[6] E. H. Shaik and R. Nakeeran, Photonic Network Commun. **39**, 15 (2020).
[7] J. H. Kim, Y. M. Jhon, Y. T. Byun, S. Lee, D. H. Woo, and S. H. Kim, IEEE Photonics Technol. Lett. **14**, 1436 (2002).
[8] Q. Liu, N. Li, and C. Tan, Phys. Rev. A **101**, 023818 (2020).
[9] V. Jandieri, R. Khomeriki, T. Onoprishvili, D. H. Werner, J. Berakdar, and D. Erni, Opt. Express **28**, 18317 (2020).
[10] N. A. Silva, T. D. Ferreira, and A. Guerreiro, New J. Phys. **23**, 023013 (2021).
[11] K. Mukherjee, K. Majhi, and A. Raja, J. Opt. **49**, 516 (2020).
[12] G. Poy, A. J. Hess, A. J. Seracuse, M. Paul, S. Žumer, and I. I. Smalyukh, Nat. Photonics **16**, 454 (2022).
[13] P. Tchofo Dinda, R. Radhakrishnan, and T. Kanna, J. Opt. Soc. Am. B **24**, 592 (2007).
[14] M. Vijayajayanthi, T. Kanna, M. Lakshmanan, and K. Murali, Commun. Nonlinear Sci. Numer. Simul. **36**, 391 (2016).
[15] M. Vijayajayanthi, T. Kanna, K. Murali, and M. Lakshmanan, Phys. Rev. E **97**, 060201(R) (2018).
[16] G. P. Agrawal, *Nonlinear Fiber Optics*, 5th ed. (Academic, San Diego, 2013).
[17] N. N. Akhmediev and A. Ankiewicz, *Solitons: Nonlinear Pulses and Beams* (Chapman & Hall, London, 1997).
[18] C. R. Menuyk, Opt. Lett. **12**, 614 (1987).
[19] C. R. Menuyk, IEEE J. Quantum Electron. **25**, 2674 (1989).
[20] P. K. A. Wai and C. R. Menyuk, J. Lightwave Technol. **14**, 148 (1996); D. Marcuse, C. R. Menyuk, and P. K. A. Wai, *ibid.* **15**, 1735 (1997).
[21] F. Baronio, M. Conforti, A. Degasperis, S. Lombardo, M. Onorato, and S. Wabnitz, Phys. Rev. Lett. **113**, 034101 (2014).
[22] S. V. Manakov, Zh. Eksp. Teor. Fiz **65**, 505 (1973) [Sov. Phys. JETP **38**, 248 (1974)].
[23] R. Radhakrishnan, M. Lakshmanan, and J. Hietarinta, Phys. Rev. E **56**, 2213 (1997).
[24] T. Kanna and M. Lakshmanan, Phys. Rev. Lett. **86**, 5043 (2001).
[25] T. Kanna and M. Lakshmanan, Phys. Rev. E **67**, 046617 (2003).
[26] T. Kanna, M. Lakshmanan, P. T. Dinda, and N. Akhmediev, Phys. Rev. E **73**, 026604 (2006).
[27] T. Kanna, K. Sakkaravarthi, and M. Vijayajayanthi, Pramana J. Phys. **85**, 881 (2015).
[28] M. Vijayajayanthi, T. Kanna, and M. Lakshmanan, Eur. Phys. J. Spec. Top. **173**, 57 (2009).
[29] Y. H. Qin, L. C. Zhao, and L. Ling, Phys. Rev. E **100**, 022212 (2019); Y. H. Qin, L. C. Zhao, Z. Q. Yang, and L. Ling, *ibid.* **104**, 014201 (2021).
[30] J. U. Kang, G. I. Stegeman, J. S. Aitchison, and N. Akhmediev, Phys. Rev. Lett. **76**, 3699 (1996).
[31] J. Fatome, I. El-Mansouri, J. Blanchet, S. Pitois, G. Millot, S. Trillo, and S. Wabnitz, J. Opt. Soc. Am. B **30**, 99 (2013).
[32] B. Frisquet, B. Kibler, J. Fatome, P. Morin, F. Baronio, M. Conforti, G. Millot, and S. Wabnitz, Phys. Rev. A **92**, 053854 (2015).
[33] B. Frisquet, B. Kibler, and P. Morin, Sci. Rep. **6**, 20785 (2016).
[34] J. Yang, Phys. Rev. E **59**, 2393 (1999).
[35] D. Miller, Nat. Photonics **4**, 3 (2010).
[36] N. Akhmediev and A. Ankiewicz, Phys. Rev. Lett. **82**, 2661 (1999).